Journal of Alloys and Compounds, *176* (1991) 123–132
JAL 0010

Single-crystal X-ray diffraction studies of $BaNb_4O_6$ and $Ba_2Nb_5O_9$

G. Svensson*, J. Köhler and A. Simon
Max-Planck-Institut für Festkörperforschung, Heisenbergstr. 1, W-7000 Stuttgart 80 (F.R.G.)

(Received April 18, 1991)

Abstract

Single crystals of $BaNb_4O_6$ (**I**) and $Ba_2Nb_5O_9$ (**II**) have been prepared by heating pellets containing $Ba_5Nb_4O_{15}$, NbO_2, NbO, Nb (Ba:Nb:O = 1:7:9 for **I** and 4:14:23 for **II** together with 10% BaF_2 as mineralizer for 24 h in a sealed niobium ampoule at 1600 °C. The crystal structures of **I** and **II** have been refined using single-crystal data (CAD 4: **I**, 128 unique reflections, $R = 1.91\%$, $R_w = 1.70\%$, **II**, 223 unique reflections, $R = 2.75\%$, $R_w = 2.55\%$). **I** crystallizes in *P4/mmm* with $a = 4.182(1)$ Å and $c = 8.212(1)$ Å and **II** in *P4/mmm* with $a = 4.172(1)$ Å and $c = 12.224(1)$ Å. The atomic positions are slightly different from those previously obtained from powder data.

The structures of **I** and **II** contain Nb_6O_{12} clusters linked to two-dimensional sheets and can be described in terms of an intergrowth between slabs of perovskite- and NbO-type structures. **I** and **II** are metallic and exhibit a weak temperature-independent paramagnetism.

1. Introduction

Among the reduced oxoniobates, phases containing isolated and condensed clusters have been synthesized [1–26]. Most of these structures can be described in terms of a common close packing of oxygen atoms, octahedral Nb_6 units and large atoms of electropositive metals. The Nb_6 units are surrounded by 12 oxygen atoms positioned outside the edges (O^i; i, *innere*) and up to 6 more oxygen atoms in front of the apices (O^a; a, *äußere*), using the terminology of Schäfer and Schnering [27]. Such Nb_6O_{12} clusters may occur discrete or condensed. So far, only condensation via vertices of the Nb_6 unit has been observed. The ultimate degree of such a type of condensation is reached in the structure of NbO [28]. It can be described as an NaCl-type structure with 25% ordered vacancies in both sublattices but also as a framework of Nb_6O_{12} clusters [27] condensed according to $Nb_{6/2}O_{12/4}$. The latter view has been substantiated by band structure calculations [29, 30].

Two-dimensional condensation has been found in phases of the type ANb_4O_6 (A = K [16, 18] and Ba [21]) and $A_2Nb_5O_9$ (A = K [16], Sr [12, 16],

---

*Permanent address: Department of Inorganic Chemistry, Stockholm University, S-10691 Stockholm, Sweden.

0925-8388/91/$3.50

Ba [12, 16, 21] and Eu [21, 26]). These structures can be described in terms of an intergrowth between slabs of perovskite- and NbO-type structures. In ANb_4O_6 the slabs are a single unit, while in $A_2Nb_5O_9$ the perovskite-type slabs are two units wide. The linkage scheme of the Nb_6O_{12} clusters is ${}^2_\infty[Nb_2Nb_{4/2}O^{i-i}_{8/2}O^{i-i}_{4/4}]O^{a-a}_{2/2}$ in ANb_4O_6 and ${}^2_\infty[Nb_2Nb_{4/2}O^{i-i}_{8/2}O^{i-i}_{4/4}]O^{a}_{2}$ in $A_2Nb_5O_9$. In the K–Nb–O and Ba–Nb–O systems both ANb_4O_6 and $A_2Nb_5O_9$ have been synthesized, which can be considered as being members of different homologous series. The compositions of these series vary as $A_nNb_{n+3m}O_{3n+3m}$ (n is the number of the perovskite-type slab, and m is the number of the NbO-type slab).

Recently one-dimensional condensation has been found in $Ba_{0.8}Nb_5O_8$ [20] and $Ba_{4-x}Nb_{17}O_{26}$ ($x \approx 1.0$) [23]. The structures contain single ($1 \times 1 \times \infty$) and quadruple ($4 \times 4 \times \infty$) chains of Nb_6O_{12} clusters corresponding to ${}^1_\infty[Nb_4Nb_{2/2}O^{i-i}_{8/2}\ O^{i-a}_{4/2}]O^{a-i}_{4/2}$ in $Ba_{0.8}Nb_5O_8$ and ${}^1_\infty[Nb_2Nb_{4/2}O^{i-i}_{5/4}O^{i-i}_{6/2}O^{i-a}_{1/2}]\ O^{a-i}_{1/2}O^{a}$ in $Ba_{4-x}Nb_{17}O_{26}$ ($x \approx 1.0$). These phases are only formed at high temperatures (about 1600 °C). At lower temperatures, '*phasoids*' [14, 19] exhibiting a disordered intergrowth between Nb_6O_{12} cluster chains or rather columns of NbO- and perovskite-type structures are found.

The use of fluorides, chlorides, borates or boron oxide (forming borates *in situ*) as mineralizers or fluxes has led to single crystals of many reduced oxoniobates containing Nb_6O_{12} clusters [1, 3–11, 17, 25]. However, oxoniobates containing one- or two-dimensionally condensed clusters have only been studied by means of profile refinement of their X-ray or neutron powder patterns. In this paper we report on the growth and X-ray investigations of single crystals of such compounds.

2. Experimental details

The starting materials used were niobium (p.a., Merck), NbO (99.9%, Alfa), NbO_2 (99.9%, Alfa), $Ba_5Nb_4O_{15}$ and BaF_2 (p.a., Merck). The latter was used as a flux–mineralizer. $Ba_5Nb_4O_{15}$ was synthesized by heating appropriate amounts of $BaCO_3$ (p.a., Merck) and Nb_2O_5 (p.a., Merck) at 1000 °C for 10 h, regrinding and reheating for another 10 h. Appropriate amounts of starting materials (compositions: Ba:Nb:O = 1:7:9 for **I** and 4:14:23 for **II**) with addition of 10% BaF_2 as mineralizer were ground together, pressed into pellets and heated in open niobium ampoules under vacuum (2×10^{-4} Torr) at 350 °C to remove any moisture. The niobium ampoules were then sealed under an argon atmosphere, heated for 24 h at 1600 °C and then cooled to 1200 °C at a cooling rate of 1 °C min whereafter the furnace was turned off. The corresponding X-ray powder patterns showed lines of $BaNb_4O_6$ (**I**) and $Ba_2Nb_5O_9$ (**II**), together with weak lines of BaF_2. The pellets contained grey plate-like crystals of **I** and **II** up to 0.1 mm exhibiting a metallic lustre. The compositions of the reaction products deviate from the starting compositions according to the phase analyses. This can be explained by the fact that BaF_2 acts not only as mineralizer but also as a barium source and niobium oxofluorides are known to be volatile at high temperatures [31].

The unit cell parameters for $BaNb_4O_6$ and $Ba_2Nb_5O_9$ (Table 1) were obtained from X-ray powder photographs (Cu $K\alpha_1$, 1.540 589 Å; Guinier–Simon technique) and were analysed using a film scanner system [32] with silicon [33] as internal standard.

When using fluorides as a flux–mineralizer for the synthesis of oxoniobates, fluorine is sometimes incorporated to some extent into the structures [5, 11, 17]. Replacement of oxygen by fluorine in oxoniobates is often followed by a change in the unit cell parameters, *e.g.* $KNb_8O_{14-x}F_x$ [17] and $K_4Al_2Nb_{11}O_{21-x}F_x$ [11]. However, since the unit cell parameters obtained for **I** and **II** are the same, within standard deviations, as those obtained without using fluoride-containing fluxes, we do not think that fluorine is present in the crystals.

Details of the single-crystal structure determinations for **I** and **II** are summarized in Table 1. In **I** two and in **II** five strong reflections showed extensive extinction and were omitted from the refinements. The atomic coordinates and thermal parameters for **I** and **II** are given in Table 2.

The positional parameters for $BaNb_4O_6$ (I) and $Ba_2Nb_5O_9$ (II) reported by Zubkov *et al.* [21] and Svensson [12, 14] and in this study are essentially in agreement. This is not surprising since the number of free parameters is rather small. However, there are some significant discrepancies. The main differences compared with the refinements from powder data are found for the position of Nb(1) in **I** [21] and the oxygen positions in **II** [12, 14].

TABLE 1

Summary of single-crystal data and X-ray intensity collection for $BaNb_4O_6$ ($Ba_2Nb_5O_9$)

Formula	$BaNb_4O_6$ ($Ba_2Nb_5O_9$)
Molar weight	605.0 amu (883.2 amu)
Lattice constants[a]	$a=4.183(1)$ Å (4.172(1) Å), $c=8.212(1)$ Å (12.224(1) Å)
Space group	*P4/mmm* (*P4/mmm*), $Z=1$ (1)
d_{calc}	6.99 g cm^{-3} (6.89 g cm^{-3})
μ(Mo $K\alpha$), λ	134.16 cm^{-1} (145.44 cm^{-1}), 0.71069 Å
Dimensions of the single crystal	0.03 mm×0.03 mm×0.02 mm (0.04 mm×0.04 mm×0.01 mm)
Data collection	Four-circle diffractometer (CAD4), graphite monochromator, scintillation counter
Range of data, method	4° (4°)$\leq 2\theta \leq$60° (60°), ω scan (ω scan)
Scan speed	variable depending on I
Number of reflections	671 (1215)
Independent	128 (223) of 671 (1214) with $F \geq 3\sigma(F)$
Absorption correction	Ψ scan with 7 (6) reflections
Refinement	SHELX program, full matrix, least squares
Number of parameters	17 (25)
R (anisotropic)	1.9% (2.7%)
R_ω (anisotropic)	1.7% (2.5%)

Further details of the crystal structure investigation may be obtained from the Fachinformationszentrum Energie, Physik, Mathematik, W-7514 Eggenstein-Leopoldshafen, F.R.G., on quoting the depository number CSD-55382, the names of the authors, and the journal citation.

[a] Modified Guinier technique.

TABLE 2

Positional parameter and U_{ij} values [$\times 10^4$] of the anisotropic temperature factors and standard deviations for $BaNb_4O_6$ (I) and $Ba_2Nb_5O_9$ (II)

Atom	Site	x	y	z	U_{11} (Å)	U_{22} (Å)	U_{33} (Å)
I							
Ba	1a	0	0	0	74(3)	74(3)	55(5)
Nb(1)	2e	0	0.5	0.5	40(3)	40(3)	40(5)
Nb(2)	2h	0.5	0.5	0.2531(1)	41(3)	41(3)	32(5)
O(1)	1b	0	0	0.5	86(23)	86(23)	204(31)
O(2)	4i	0.5	0	0.2431(7)	116(22)	90(22)	133(25)
O(3)	1c	0.5	0.5	0	126(24)	126(24)	72(30)
II							
Ba	2g	0	0	0.1681(1)	94(2)	94(2)	66(3)
Nb(1)	2e	0	0.5	0.5	66(4)	65(4)	50(4)
Nb(2)	2h	0.5	0.5	0.3364(1)	62(3)	62(3)	45(5)
Nb(3)	1c	0.5	0.5	0	71(4)	71(4)	39(6)
O(1)	1b	0	0	0.5	55(22)	55(22)	105(29)
O(2)	4i	0.5	0	0.3271(5)	91(21)	136(22)	125(23)
O(3)	2h	0.5	0.5	0.1596(7)	110(20)	110(20)	204(28)
O(4)	2f	0	0.5	0	158(26)	109(25)	137(26)

The U_{ij} are defined for $\exp\{-2\pi 2\,(U_{11}h^2a^{*2} + \cdots + 2U_{23}klb^*c^*)\}$. $U_{12} = U_{13} = U_{23} = 0$ for all barium, niobium and oxygen atoms in both compounds.

Electrical conductivity measurements between 300 K and 4 K on **II** (ceramic sample prepared according to ref. 12) show it to be metallic. **I** has also been found to be metallic [24].

Measurements of the magnetic susceptibility on $BaNb_4O_6$ (I) and $Ba_2Nb_5O_9$ (II) (both containing a small amount of BaF_2; see above) have been performed between 3.6 and 300 K in a superconducting quantum interference device magnetometer employing a field of 10 kG. **I** and **II** both exhibit a weak temperature-independent paramagnetism of $245(10) \times 10^{-6}$ e.m.u. mol^{-1} and $195(10) \times 10^{-6}$ e.m.u. mol^{-1} respectively (uncorrected for the diamagnetic contribution).

3. Description of the structures

The structures of $BaNb_4O_6$ **I** and Ba_2Nb_5 (**II**) are shown in Fig. 1. Interatomic distances are given in Table 3. Patterns of the mutual adjunction [34] together with bond order sums [35] are summarized in Table 4.

At first sight, the structure of **I** is composed of NbO-type layers alternating with intermediate BaO layers while the structure of **II** contains alternating slabs of NbO and perovskite types. This view is somewhat too simplified as the interactions between the slabs are not taken into account. The atoms in the BaO layer in **I** are surrounded by nearest neighbours as in a perovskite structure. Therefore, a description of the structure in terms of an intergrowth

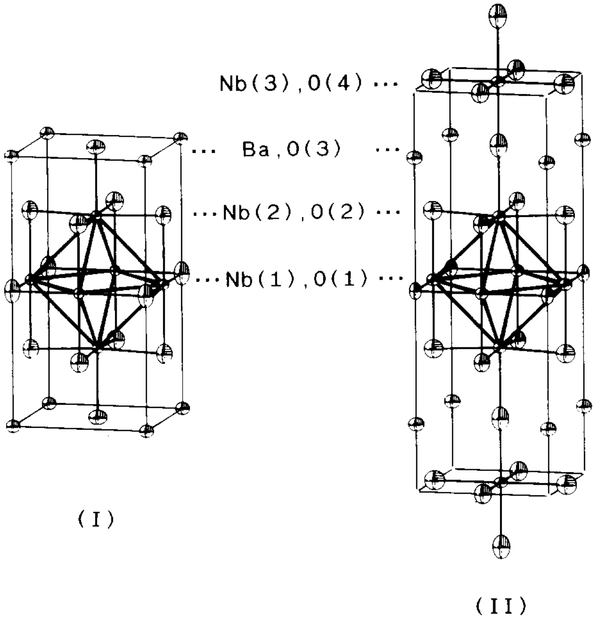

Fig. 1. ORTEP drawing of the structures of $BaNb_4O_6$ (I) and $Ba_2Nb_5O_9$ (II). The ellipsoids have been drawn with a probability of 90%.

TABLE 3

Important interatomic distances (Ångströms) in $BaNb_4O_6$ (I) and $Ba_2Nb_5O_9$ (II)

I							
Ba	O(2)	2.891(4)	(8×)	Nb(1)	O(1)	2.091(1)	(2×)
	O(3)	2.958(1)	(4×)		O(2)	2.110(6)	(2×)
					Nb(2)	2.913(1)	(4×)
					Nb(1)	2.958(1)	(4×)
Nb(2)	O(3)	2.078(1)					
	O(2)	2.093(1)	(4×)				
	Nb(1)	2.912(1)	(4×)				
II							
Ba	O(2)	2.852(4)	(4×)	Nb(2)	O(2)	2.089(1)	(4×)
	O(4)	2.928(1)	(4×)		O(3)	2.161(9)	
	O(3)	2.952(1)	(4×)		Nb(1)	2.890(1)	(4×)
Nb(1)	O(1)	2.086(1)	(2×)				
	O(2)	2.113(6)	(2×)				
	Nb(2)	2.890(1)	(4×)	Nb(3)	O(3)	1.951(9)	(2×)
	Nb(1)	2.950(1)	(4×)		O(4)	2.086(1)	(4×)

of one NbO-type and one perovskite-type slab with boundary atoms being shared between different slabs seems more appropriate, particularly because this description emphasizes the intimate structure relationship of **I** to **II**, the perovskite type slabs being one and two units wide for **I** and **II** respectively.

TABLE 4

Motifs of the mutual adjunction [34] and bond order sums Σs_i [35] in $BaNb_4O_6$ (**I**) and $Ba_2Nb_5O_9$ (**II**)

Atom	$1\times O(3)^{a-a}$	$4\times O(2)^{i-i}$	$1\times O(1)^{i-i}$	CN	Σs_i
I					
1×Ba	4/4	8/2	–	12	2.21
2×Nb(1)	–	2/1	2/4	4	2.40
2×Nb(2)	1/2	4/2	–	5	3.08
CN	6	5	4		
Σs_i	1.92	2.20	2.46		

Atom	$2\times O(4)$	$2\times O(3)^{a}$	$4\times O(2)^{i-i}$	$1\times O(1)^{i-i}$	CN	Σs_i
II						
2×Ba	4/4	4/4	4/2	–	12	2.23
2×Nb(1)	–	–	2/1	2/4	4	2.40
2×Nb(2)	–	1/1	4/2	–	5	2.98
1×Nb(3)	4/2	2/1	–	–	6	4.29
CN	6	6	5	4		
Σs_i	1.95	2.07	2.25	2.49		

CN, coordination number.

In both structures the barium atoms have a coordination number of 12, as in $Ba_{0.95}NbO_3$ [36–39], forming a distorted cube–octahedron. The Ba–O bonding distances are in the ranges 2.891–2.958 Å for $BaNb_4O_6$ (**I**) and 2.852–2.952 Å for $Ba_2Nb_5O_9$ (**II**), in close agreement with the Ba–O distance of 2.889 Å in $Ba_{0.95}NbO_3$. The coordination octahedron around Nb(3) is tetragonally compressed (4×2.086 Å and 2×1.951 Å).

In **I** and **II**, Nb(1) and Nb(2) in the NbO-type slabs form Nb_6 octahedra coordinated by oxygen atoms to form clusters of the M_6X_{12} type. These octahedra are also tetragonally compressed. In **I**, $d_{Nb(2)-Nb(2)} = 4.056$ Å compared with $d_{Nb(1)-Nb(1)} = 4.182$ Å and, in **II**, $d_{Nb(2)-Nb(2)} = 4.000$ Å compared with $d_{Nb(1)-Nb(1)} = 4.172$ Å.

The interatomic distances between the Nb(1) atoms having a strictly planar coordination of oxygen atoms are 2.958 Å and 2.950 Å for $BaNb_4O_6$ (**I**) and $Ba_2Nb_5O_9$ (**II**) respectively. These niobium atoms have an environment similar to that found in NbO. The Nb(2) atoms are shared between the perovskite- and the NbO-type slabs and have a fivefold coordination of oxygen atoms as found for niobium atoms in compounds with discrete Nb_6O_{12} clusters. The Nb(1)–Nb(2) distances (2.913 Å for **I**, 2.890 Å for **II**) are somewhat shorter than those between the Nb(1) atoms. The O(2)–Nb(2)–O(2) angles are 175.5° (**I**) and 173.8°, (**II**) compared with the planar coordination around Nb(1).

The Nb–O^i distances are 2.091–2.110 Å (**I**) and 2.086–2.161 Å (**II**), similar to those usually found for discrete Nb_6O_{12} clusters.

In both structures the coordinations of the oxygen atoms are similar: O(1) is square planar surrounded by four niobium atoms as in NbO, O(2) is coordinated by two barium and three niobium atoms and, O(3) and O(4) (in **II**) are coordinated by four barium and two niobium atoms as in $Ba_{0.95}NbO_3$.

4. Discussion

$BaNb_4O_6$ (**I**) and $Ba_2Nb_5O_9$ (**II**) represent ordered intergrowth structures between NbO and $BaNbO_3$. Bulk crystals of NbO ($a = 4.2101$ Å [28]) and $Ba_{0.95}NbO_3$ ($a = 4.085$ Å [36–39]) exhibit a significant lattice constant difference and an epitaxial composite crystal of both would build up considerable strain owing to this mismatch. Layerwise intergrowth obviously allows for strain relief by mutual adjustment of the different kinds of slabs. Atomic shifts in the stacking direction enter as an additional degree of freedom for this adjustment.

The a lattice constants of **I** and **II** closely correspond to the value for NbO, not unexpected in view of the rigid bonding within the cluster framework. The Nb_6 octahedra are flattened by 3%–4% owing to the weaker bonding of the niobium atoms into the perovskite-type slabs compared with bulk NbO. On the contrary, the perovskite-type slabs are (compared with bulk $Ba_{0.95}NbO_3$) stretched by approximately 2% in the C plane and, referring to the position of O(2), contracted by approximately 2% along c. As a consequence, the cube octahedra of oxygen atoms around barium is compressed along the c axis to the same extent. The remarkable distortion of the octahedron of oxygen atoms around Nb(3) is a result of the overall strain relief in the structures.

The oxidation state of Nb(3) is disputable. An extended Hückel band structure calculation for $Ba_2Nb_5O_9$ seemed to answer that question unambiguously. This calculation [40] was based on the preliminary atomic positions [12] which deviate significantly, in particular for the position of O(2), from the now available single-crystal data. The calculation showed the rather dispersionless Nb(3)-based d bands (t_{2g} character) to lie above the Fermi level at the electron count of $Ba_2Nb_5O_9$, thus indicating a pentavalent Nb(3).

Bond order calculations have been performed repeatedly for reduced oxoniobates to derive oxidation states for different kinds of niobium atoms, *e.g.* in ref. 5. If such calculations are applied for Nb(3) in **II**, with bond order sums for O(4) and O(3) of 2.07 and 1.95 respectively, the value of 4.29 for Nb(3) is in the same range as for the niobium atoms in $Ba_{0.95}NbO_3$ (4.24) and NbO_2 (α [41], 4.26 and 4.16; β [42], 4.27 and 4.03) giving an indication for tetravalent niobium, although one has to be careful in assigning oxidation states for bond order summations.

Actually the compounds discussed here serve as good examples. The bond order sums for barium are nearly the same for both compounds, 2.21 for **I** and 2.23 for **II**. Although they are in close agreement with one another and with the value of 2.37 for $Ba_{0.95}NbO_3$, they deviate from the expected value 2.0 (in BaO the bond order sum for barium is 1.66). The bond order sums for O(1) in **I** and **II** are 2.46 and 2.49 respectively, close to the value for the oxygen, atom in NbO (2.41) but again dramatically deviating from the expected value 2.0.

To shed more light on the oxidation state of Nb(3), we have performed Madelung part of lattice energy (MAPLE) calculations [43, 44] for $BaNb_4O_6$ (I) and $Ba_2Nb_5O_9$ (**II**) (Table 5). Usually the MAPLE value of a ternary oxide should not deviate by more than 1% from the sum of the MAPLE values of the corresponding binary oxides or ternary components. However, such a calculation is only meaningful if the structural elements are comparable. **II** can be considered as an intergrowth of **I** and $BaNbO_3$ but, as the latter is only known to exist as $Ba_{0.95}NbO_3$ [39], we took BaO and NbO_2 as the reference compounds instead.

A theoretical MAPLE value X is calculated for $Ba_2Nb_5O_9$ (**II**) according to

$$\mathrm{MAPLE}(BaNb_4O_6) + \mathrm{MAPLE}(NbO_2) + \mathrm{MAPLE}(BaO) = X$$

$$5962.6 + 3071.7 + 839.9 = 9874.2 \text{ kcal mol}^{-1}$$

MAPLE($Ba_2Nb_5O_9$) has been calculated assuming that the number of valence electrons for the cluster sheet in **II** is 10, as in **I**, and the oxidation state for Nb(3) is +4; see Table 5. It deviates only by 0.5% from X, which means that the cluster sheets in **I** and **II** are comparable. Since no compound containing such a cluster sheet with 11 valence electrons is known, we cannot perform such a comparison with a pentavalent Nb(3).

TABLE 5

Contribution of atoms to the Madelung part of lattice energy in $BaNb_4O_6$ (I) and $Ba_2Nb_5O_9$ (II)

I				**II**			
Atom		MAPLE	Σ MAPLE	Atom		MAPLE	Σ MAPLE
Ba	1×	617.6	617.6	Ba	2×	576.8	1153.6
Nb(1)	2×	455.0	910.0	Nb(1)	2×	327.1	654.2
Nb(2)	2×	789.2	1578.4	Nb(2)	2×	662.5	1325.5
O(1)	1×	713.5	713.5	Nb(3)	1×	2384.8	2384.8
O(2)	4×	471.9	1887.6	O(1)	1×	816.5	816.5
O(3)	1×	255.5	255.5	O(2)	4×	561.3	2245.2
				O(3)	2×	342.7	685.4
				O(4)	2×	328.0	656.0
Sum			5962.8	Sum			9920.6

The following charge distributions have been used:

I Ba, +2; Nb(1), +2.5; Nb(2), +2.5; O(1)· · ·O(3), -2

II Ba, +2; Nb(1), +2.5; Nb(2), +2.5; Nb(3), +4; O(1)· · ·O(4), -2

If Nb(3) is assumed to be tetravalent, the number of valence electrons available for Nb–Nb bonding within the cluster sheet is 2.5 per niobium atom in both $BaNb_4O_6$ (**I**) and $Ba_2Nb_5O_9$ (**II**). Obviously the electron count can vary within certain limits as it is observed that KNb_4O_6 and $K_2Nb_5O_9$ exist in both of the corresponding structure types. At considerably higher electron counts another structure is formed which is also based on condensed M_6O_{12} clusters, yet in a different mode of condensation. Thus in the structure of KMo_4O_6 [45] (isotypic with $NaMo_4O_6$ [46], 3.25 electrons per M atom) chains of *trans*-edge-sharing Mo_6 octahedra occur.

5. Conclusion

We have synthesized single crystals of $BaNb_4O_6$ and $Ba_2Nb_5O_9$ using BaF_2 as flux–mineralizer. The structures of these phases are intergrowth types, consisting of alternating layers of perovskite type and NbO type. They can thus be considered as members of a homologous series $A_nNb_{n+3m}O_{3n+3m}$ where $BaNb_4O_6$ has $n=m=1$ and $Ba_2Nb_5O_9$ $n=2$ and $m=1$.

Acknowledgments

We wish to thank Dr. Magnus Ekelund and Dr. Kjell Jansson at the Department of Inorganic Chemistry, Stockholm University, for the thermal treatment of the samples. We also wish to thank E. Brücher for the measurement of the magnetic susceptibilities. Gunnar Svensson also wishes to thank the Alexander von Humboldt Stiftung for the stipendium making his visit to the Max Planck Institute für Festkörperforschung in Stuttgart possible.

References

1 D. M. Evans and L. Katz, *J. Solid State Chem.*, *6* (1973) 459.
2 B. O. Marinder, *Chim. Scr.*, *11* (1977) 97.
3 J. Köhler and A. Simon, *Angew. Chem.*, *98* (1986) 1011; *Angew. Chem., Int. Edn. Engl.*, *25* (1986) 996.
4 R. Burnus, J. Köhler and A. Simon, *Z. Naturforsch.*, *426* (1987) 536.
5 J. Köhler and A. Simon, *Z. Anorg. Allg. Chem.*, *553* (1987) 106.
6 S. J. Hibble, A. K. Cheetham and D. E. Cox, *Inorg. Chem.*, *26* (1987) 2389.
7 J. Köhler, A. Simon, S. J. Hibble and A. K. Cheetham, *J. Less-Common Met.*, *142* (1988) 123.
8 J. Köhler, G. Miller and A. Simon, *Z. Anorg. Allg. Chem.*, *568* (1989) 8.
9 J. Köhler and A. Simon, *Z. Anorg. Allg. Chem.*, *572* (1989) 7.
10 S. J. Hibble, A. K. Cheetham, J. Köhler and A. Simon, *J. Less-Common Met.*, *154* (1989) 271.
11 J. Köhler, A. Simon, R. Tischtau and G. Miller, *Angew. Chem.*, *101* (1989) 1695; *Angew. Chem. Int. Edn. Engl.*, *28* (1989) 1662.
12 G. Svensson, *Mater. Res. Bull.*, *23* (1988) 437.
13 G. Svensson, *J. Solid State Ionics*, *32-33* (1989) 126.

14 G. Svensson, *Chem. Commun. Stockholm Univ.*, *3* (1989) 1.
15 G. Svensson, *Acta Chem. Scand.*, *44* (1990) 222.
16 C. E. Michelson, P. E. Rauch and F. J. DiSalvo, *Mater. Res. Bull.*, *25* (1990) 971.
17 J. Köhler, R. Tischtau and A. Simon, *J. Chem. Soc., Dalton Trans.*, (1991) 829.
18 G. Svensson, *J. Solid State Chem.*, *90* (1991) 249.
19 G. Svensson, *Microsc. Microanal. Microstruct.*, *1* (1990) 343.
20 V. G. Zubkov, V. A. Perelyayev, I. F. Berger, I. A. Kontzevaya, O. B. Makarova, S. A. Turshevskii, V. A. Gubanov, V. I. Voronin, A. V. Mirmelstein and E. A. Karkin, *Sverkhprovod. Fiz., Khim., Tekhonol.*, *3* (9) (1990) 2121.
21 V. G. Zubkov, V. A. Perelyayev, I. F. Berger, V. I. Voronin, I. A. Kontzevaya and G. P. Shveikin, *Dokl. Akad. Nauk S.S.S.R., Kristallogr.*, *312* (3) (1990) 615.
22 V. G. Zubkov, V. A. Perelyayev, D. G. Kellermann, V. E. Stapsev, V. P. Lyankina, I. A. Kontzevaya, O. B. Makarova and G. P. Sveikin, *Dokl. Akad. Nauk S.S.S.R.*, *313* (2) (1990) 361.
23 V. G. Zubkov, V. A. Perelyayev and G. P. Shveikin, to be published.
24 S. A. Davydov, B. N. Goschchitskii, E. A. Karkin, A. V. Mirmelstein, V. I. Voronin, V. D. Parkhomenko, V. G. Zubkov, V. A. Perelyayev, I. F. Berger and I. A. Kontzevaya, *Int. J. Mod. Phys. B*, *4* (1990) 1531.
25 K. B. Kersting and W. Jeitschko, *Acta Crystallogr. A*, *46* (Suppl. C) (1990) 262.
26 J. Köhler, to be published.
27 H. Schäfer and H. G. Schnering, *Angew. Chem.*, *76* (1964) 833.
28 G. Brauer, *Z. Anorg. Allg. Chem.*, *248* (1941) 1.
29 O. K. Andersen and S. Satpathy, in A. Dominguez, J. Castaing and R. Marquez (eds.), *Basic Properties of Binary Oxides*, Serv. Publ. Univ. Sevilla, 1983, p. 21.
30 J. K. Burdett and T. Hughbanks, *J. Am. Chem. Soc.*, *106* (1984) 3103.
31 S. Andersson and A. Åström, *Acta Chem. Scand.*, *19* (1965) 2136.
32 K. E. Johansson, T. Palm and P.-E. Werner, *J. Phys. E*, *13* (1980) 1298.
33 C. R. Hubbard, H. E. Swanson and F. A. Mauer, *J. Appl. Crystallogr.*, *8* (1975) 45.
34 R. Hoppe, *Angew. Chem.*, *92* (1980) 25; *Angew. Chem., Int. Edn. Engl.*, *19* (1980) 110.
35 I. D. Brown and D. Altermatt, *Acta Crystallogr. B*, *41* (1985) 244.
36 D. Ridgley and R. Ward, *J. Am. Chem. Soc.*, *77* (1955) 6132.
37 R. Kreiser and R. Ward, *J. Solid State Chem.*, *1* (1970) 368.
38 G. Svensson and P.-E. Werner, *Mater. Res. Bull.*, *25* (1990) 9.
39 B. Hessen, S. A. Sunshine, T. Siegrist and R. Jimenez, *Mater. Res. Bull.*, *26* (1991) 85.
40 G. Miller, personal communication, 1988.
41 R. Pynn, J. D. Axe and R. Thomas, *Phys. Rev. B*, *13* (1976) 2965.
42 H. J. Schweizer and R. Gruehn, *Z. Naturforsch. B*, *37* (1982) 1361.
43 R. Hoppe, *Angew. Chem.*, *78* (1966) 52; *Angew. Chem., Int. Edn. Engl.*, *5* (1966) 95.
44 R. Hoppe, *Adv. Fluorine Chem.*, *6* (1970) 387.
45 R. Hoffman, R. Hoppe, K. Bauer and K. J. Range, *J. Less-Common Met.*, *161* (1990) 279.
46 C. C. Torardi and R. E. McCarley, *J. Am. Chem. Soc.*, *101* (1979) 3963.